Extended Abstract

13th International ASTM/ESIS Symposium on Fatigue and Fracture Mechanics, (39th National Symposium on Fatigue and Fracture Mechanics), Jacksonville, Florida

Experimental Characterization and Simulation of Slip Transfer at Grain Boundaries and Microstructurally-Sensitive Crack Propagation

Vipul Gupta[1,*], Jacob Hochhalter[2], Vesselin Yamakov[1], Scott Willard[3], Ashley Spear[4], Stephen Smith[2] and Edward Glaessgen[2]

[1]National Institute of Aerospace, Hampton, VA 23666
[2]NASA Langley Research Center, Hampton, VA 23681-2199
[3]Science and Technology Corporation, Hampton, VA 23666
[4]Cornell University, Ithaca, NY 14853-6413

Abstract

A systematic study of crack tip interaction with grain boundaries is critical for improvement of multiscale modeling of microstructurally-sensitive fatigue crack propagation and for the computationally-assisted design of more durable materials. In this study, single, bi- and large-grain multi-crystal specimens of an aluminum-copper alloy are fabricated, characterized using electron backscattered diffraction (EBSD), and deformed under tensile loading and nano-indentation. 2D image correlation (IC) in an environmental scanning electron microscope (ESEM) is used to measure displacements near crack tips, grain boundaries and within grain interiors. The role of grain boundaries on slip transfer is examined using nano-indentation in combination with high-resolution EBSD. The use of detailed IC and EBSD-based experiments are discussed as they relate to crystal-plasticity finite element (CPFE) model calibration and validation.

*Corresponding Author. Address: 100 Exploration Way, Hampton, VA 23666-6147, USA. Tel: +1 (757) 864 6355, Fax: +1 (757) 864 8911; Email: vipul.gupta@nianet.org.

1. Introduction

Design and development of new engineering materials, as well as utilizing current materials for new applications, rely on establishing high fidelity computational models that link materials processing, microstructure and properties at various length scales. Without complete access to experimental data at the appropriate length scales, computational model predictions of complex phenomena, e.g. microstructurally-sensitive small fatigue crack initiation and propagation, remain elusive.

In recent years, several polycrystal models have been developed to simulate constitutive behavior, which rely on the calibration of material parameters [1-3]. In the case of polycrystalline materials, finite-element (FE) models are often constructed with the help of optical and/or EBSD data of the grain morphology [4]. At the microstructural-level, the importance of material heterogeneities increases, and the local microstructural behavior can be significantly different from the average materials behavior [5]. In this case, the model has to account for the microstructural details such as local grain structure, texture and compositional

changes. Crystal plasticity-based finite element (CPFE) simulations have been carried out to investigate deformation of polycrystalline aggregates [6], however, comparisons between model predictions and experimentally observed behavior have largely been done at the grain level.

To understand and predict the behavior correctly, microstructurally-based computational model simulations and experiments need to be compared locally, e.g., throughout individual grains in a polycrystalline specimen. For this purpose, detailed local experiments to quantify microstructure-level deformation are necessary. In recent years, an optical-imaging system based image correlation (IC) method with full-field measurements capabilities has emerged for quantitative local characterizations of the deformation behavior of grains and near crack tips, including crack opening profiles in a wide variety of metallic materials [7-11].

More recently, in-situ mechanical testing within scanning electron microscopes (SEM) has been used to extract quantitative information on deformation and fatigue cracking in addition to imaging during testing in a variety of materials [12-15]. The IC technique combined with in-situ testing in SEM is emerging as an ideal method for displacement measurements at the microstructural scale and for investigating deformation mechanisms such as the strains accommodated within grains, near grain boundaries, around micro-scale constituents, and at the tip of a crack in engineering material.

It is important to note that, while detailed deformation and texture measurements can be made on the surface grains of poly-crystalline samples, the effects of sub-surface grain deformation and grain boundary interactions may not be easily assessed [16]. The large-grain multi-crystals allow grain scale heterogeneity phenomena to be amplified from the microstructural-scale to conceivable level [2,6,17-19]. The current study attempts to link experimental observations with the CPFE modeling by fabricating single, bi- and large-grain multi- crystal specimens of Al-Cu alloys. The large-grain samples can also be used to test a wide variety of orientations using nano-indentation to examine the role of grain boundary on slip accumulation and transmission [20].

This paper presents SEM-based full-field IC results of grain and crack tip deformation in Al-Cu alloys to determine the data needed to calibrate and validate CPFE models for prediction of fatigue damage. It is shown that the SEM-based IC has the advantage of full-field capability giving local fidelity such as strain heterogeneities near grain boundaries, triple junctions and crack tips that can be used to guide and validate (critical concepts and observed behavior) simulation predictions by CPFE models. The goal of the study is to develop a better understanding of the slip transmission behavior in Al-Cu alloys, which may enable design of durable and damage tolerant materials with improved fatigue crack growth resistance.

2. Experimental and Methods

Precipitation hardenable Al-2wt%Cu and Al-4wt%Cu alloys (in solution treated and naturally aged condition) are used. Ingots are prepared by melting >99.99% purity Al and Cu pellets in a vacuum induction melter. A portion of each ingot is grown into a single or a bi-crystal panel from seed crystals of predefined orientations using a vertical Bridgman furnace. Large-grain multi-crystal panels are obtained by vacuum hot-pressing (VHP) a portion of an Al-Cu ingot. Mechanical test specimens in dog-bone tensile (DBT) and single edge-notch (SEN)

configurations are cut using electro-discharge machining (EDM). The dimensions of specimens used in these experiments are shown in Fig. 1.
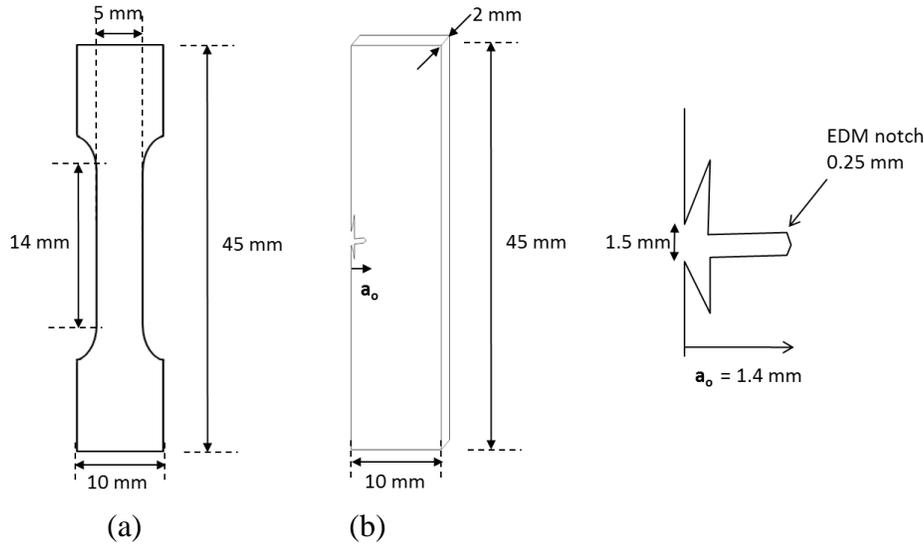

Figure 1: Schematics of (a) dog-bone tensile (DBT) specimen, and (b) single-edge notch (SEN) fatigue specimen with a detailed geometry of EDM notch.

The specimens are ground using 240–1200 grit SiC papers followed by polishing with 3, 1 and 0.25 μm petroleum distillates-based diamond suspensions and 0.02 μm non-crystalline colloidal silica suspension. Prior to mechanical testing, crystallographic orientations of test specimens are measured using an EBSD system installed in a Zeiss EVO-60® SEM equipped with a TSL EDAX® CCD camera and OIM® 6.0 software package.

Nano-indentation is performed using an MTS Nano-indenter XP® with TestWorks® data acquisition and analysis software equipped with a Berkovich diamond tip. The continuous stiffness measurement (CSM) technique is used to measure hardness, which allows for hardness data to be obtained as a continuous function of indentation depth. Indentations are conducted at several locations near selected grain boundaries and grain interiors to investigate potential grain orientation and grain boundary effect on hardness and modulus at various distances from the grain boundaries.

Image Correlation - Specimen Preparation and Displacement Measurements

Image correlation (IC) computes displacements by tracking individual subsets of a speckle pattern and determines the best correlation between the two images [8]. Speckle patterns with a non-uniform distribution of gray scale are obtained by painting the surface with a thin layer of white spray paint and then applying a black mist of spray paint to create the black speckles. This method provides a quick, cost-effective method of random pattern speckling on the large test specimens. However, the speckle feature size may vary from 20 to 200 μm, which can negatively affect the displacement resolution.

The optical image correlation (O-IC) analysis is conducted by utilizing commercial IC post-processing and data analysis software VIC-3D® (Correlated Solutions Inc., Columbia, SC).

The DBT specimens are uniaxially loaded on a mechanical test frame under constant displacement rate. Images are acquired using two 5 MP cameras. The first two images are captured at "zero" load, and used as the reference images for the full-field IC analysis. At each correlated point, displacements are calculated and differentiated to obtain the strains (Lagrange) assuming a small strain approximation in the software.

In order to obtain microstructural-level information, surface patterning (with sub-micron feature sizes ranging from 0.1 to 2 μm) using electron beam (e-beam) lithography in an SEM is performed. During the e-beam exposure process in an SEM, the spin-coated poly-methyl-meth-acrylate (PMMA) resist at the random pattern locations comes into direct contact with the e-beam and is broken up into fragments that could be easily dissolved in a developer (Methyl-Iso-Butyl-Ketone and Iso-Propyl-Alcohol in proportions of 1:3 by volume).

The SEM-based image correlation (SE-IC) measurements are conducted utilizing an in-situ load-frame installed in an ESEM. Since images are acquired in the ESEM utilizing a single secondary electron (SE) detector, the SE-IC is limited to 2D displacement measurements. For the SE-IC, spatial distortion removal is performed using a methodology that employs a series of in-plane rigid body motions. Drift distortion removal is performed using multiple, time-spaced images to extract the time-varying relative displacement field throughout the experiment. The details on calibration and drift/distortion correction can be found elsewhere [21,22]. The SEN specimens are uniaxially-loaded in an in-situ screw-driven load-frame, installed in the ESEM. For full-field IC analysis, multiple time-spaced image pairs are acquired.

3. Results and Discussion

IC-based full-field displacement measurements combined with EBSD provide information needed to characterize deformation behavior. The current results demonstrate the applications of both optical and SEM-based image correlation, and are discussed as they relate to crystal-plasticity finite element (CPFE) model calibration and validation.

Full-field Deformation Measurements using Image Correlation

3D optical image correlation (O-IC) based full-field strain maps (Fig. 2b) along with the initial grain orientation distribution map (Fig. 2a), provide the global stress-strain behavior, along with local grain-to-grain strain variation, which is necessary for CPFE model calibration and validation. For the development of high fidelity CPFE models of microstructurally-sensitive fatigue cracking, the calibration and validation require high-resolution characterization and measurements of grain-level and crack tip strain at the micron and sub-micron length scale. However, detailed strain distribution within a grain, near a grain boundary or a crack tip cannot be obtained with this macro-scale O-IC technique.

The heterogeneous deformation in the grain interiors and near grain boundaries and triple junctions are examined for the same specimen using 2D SE-IC (Fig. 2c). Note the significant reorientation taking place in grains (highlighted by black and red broken lines before and after loading, respectively). During reorientation, these grains become more favorably oriented for slip, resulting in eased plastic deformation. Moreover, the number of active slip systems with relatively high Schmid factors (≥0.4) within each grain is determined from corresponding grain

orientations which corresponded well to the extent of strain heterogeneities observed in these grains. The largest reorientation/deformation is observed in regions where the Schmid factor is the highest. The variety of inherent sources of material heterogeneity including grain anisotropy result in heterogeneous deformation fields within each grain.
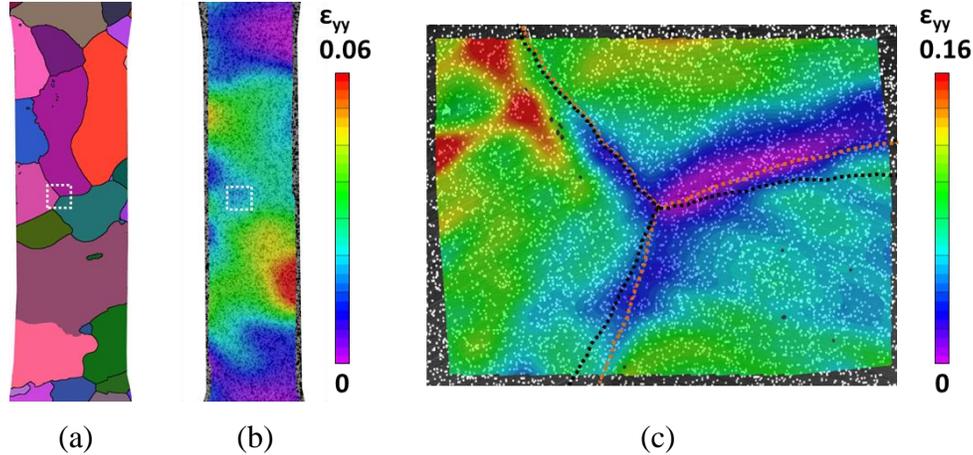

(a)   (b)   (c)

Figure 2: (a) EBSD orientation map of the gauge section of a DBT specimen of Al-4Cu alloy, (b) full field strain map measured by 3D O-IC, (c) grain-to-grain and grain boundary strain localization near a triple junction measured by 2D SE-IC. Black and red broken lines depict location of grain boundaries before and after loading, respectively.

Comparison with CPFE-based Simulation Results

A CPFE model is employed for simulation of the microstructure-level deformation for comparison with experiment. The constitutive model employed is detailed in the ref. [3]. A replicated FE model (Fig. 3d) is obtained from the experimentally determined 2D grain morphology (Fig. 3a) via direct extrusion of the specimen shape and grain morphology into the third dimension. It is assumed that this extrusion is sufficiently accurate given that the grain sizes are much larger than the specimen thickness. The materials parameters for the CPFE model are calibrated by matching the experimental macroscopic (specimen-level) engineering stress-strain response, and then the simulation results are compared with experimental surface strains, measured with IC (Figs. 3b and 3c).

The replicated CPFE model simulated strain and experiment show similar regions of strain localization across most of the specimen surface. However, there are certainly regions where significant discrepancies exist. It is observed that these discrepancies are often related to grain boundary cracking, which is not incorporated in the CPFE simulation. Although the specimen used in this study is a large-grain multi-crystal with millimeter-sized grains, the possibility of grain size variation through the thickness cannot be entirely eliminated. This represents one source of discrepancy between the experimental and simulation results to be discussed below. A second assumption made is that the local lattice orientation and material properties do not vary within the grains as well as in the specimen thickness direction. Third, grain boundaries are often sources of critical damage nucleation, which is also not captured in the CPFE model.
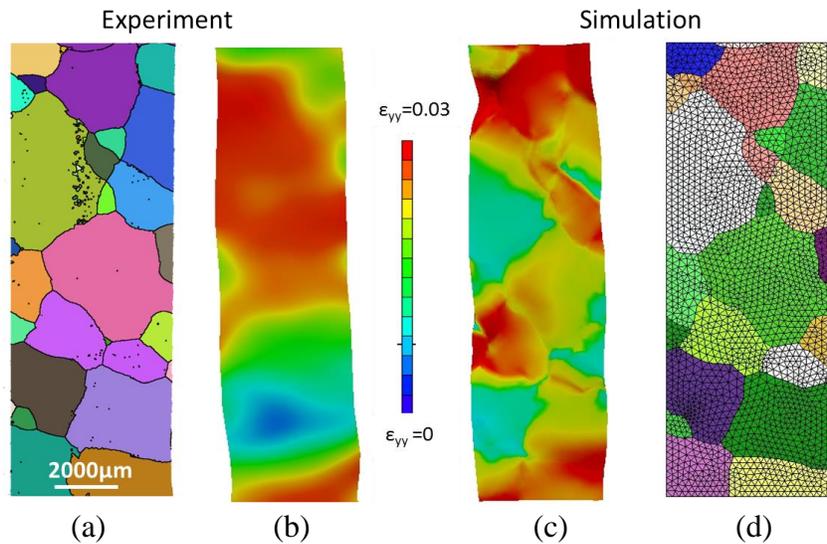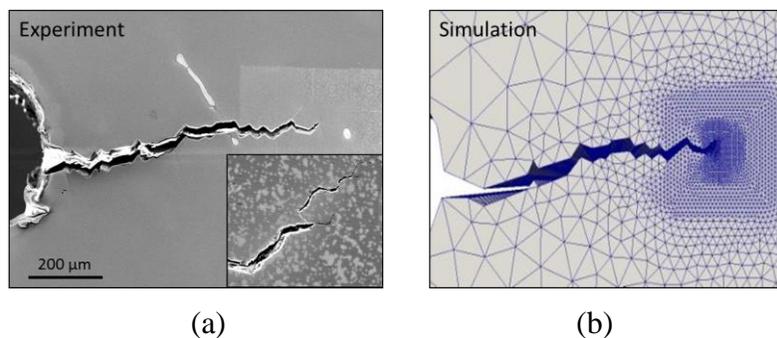
Figure 3: Comparison between experimentally measured and simulation strain results obtained from a DBT specimen of Al-4Cu alloy: (a) initial grain orientations in the specimen's gage section, (b) full-field strain map obtained through 3D O-IC, (c) CPFE model simulation results of accumulated strain, and (d) replicated FE model of experimentally measured microstructure.

Measurements of Crack Tip Strain Field in a Single Crystal Specimen

In-situ SE-IC is employed to measure the evolution of strain within a small area near a sharp crack tip in a fatigue pre-cracked SEN specimen of Al-2Cu alloy (Fig. 4a). Figure 4c shows the full-field strain map superimposed on an e-beam patterned SE image. The specimen is tested in a solutionized and naturally aged condition and; therefore, it contained shearable precipitates, allowing strain to localize during loading and eventually crack along slip-bands. A replicated CPFE model is generated (Fig. 4b), where the measured single crystal orientation and fatigue pre-crack are used to define the model. The first cycle after fatigue pre-cracking is simulated (Fig. 4d). The simulation predicts similar strain distribution and location to the measured values. In both experiment and simulation, it is evident that strain localization occurred at a secondary crack tip, near the main crack tip. This secondary crack tip is also where the fatigue crack grew during the cycle. However, as is the case with the oligo-crystal above, the replicated CPFE is generated by extruding the fatigue pre-crack which is observed on the surface. X-Ray micro-CT data of this same specimen revealed, later, that the crack face is highly non-planar through the thickness, which will be incorporated into future modeling attempts.

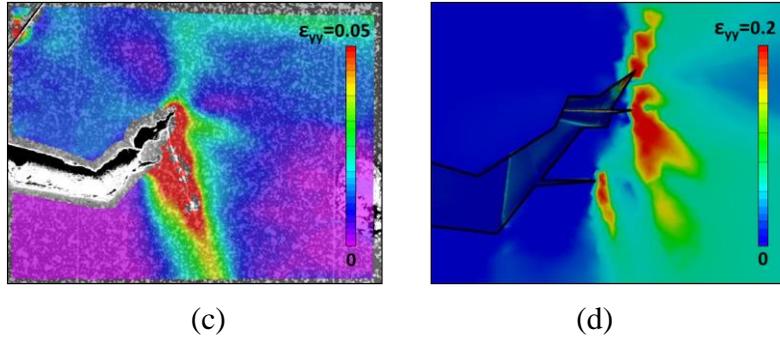(c)   (d)

Figure 4: Comparison between experimentally measured and simulation strain results obtained from a single crystal SEN specimen of Al-2Cu alloy: (a) SE image of a fatigue pre-cracked and IC-tested specimen, (b) replicated FE model of the crack path, (c) full-field strain map superimposed on the SE image, and (d) CPFE model simulation results of accumulated strain.

Role of Grain Boundary on Slip Transmission

Nano-indentation tests are conducted on single/bi- crystals and large-grain multi-crystal samples of Al-Cu alloys. Using the EBSD orientation mapping, grain boundary misorientations are measured and the favored slip systems are identified, assuming Schmid behavior as a first approximation. EBSD reference orientation-based misorientation [23], is used to image the zone of "significant plastic strain" about an indent. If a grain boundary is to produce an observed strengthening effect (i.e., blocking dislocations), a zone of significant plastic strain will be discontinuous near a grain boundary. From the EBSD misorientation map (Fig. 5), it is apparent that the dislocations are blocked by a high-angle (>15°) grain boundary as indicated by discontinuity in local lattice rotation. This correlates well with the Hall–Petch relationship which implies that grain boundaries, on average, have an inherent resistance to slip transfer, thus relating grain boundary strengthening to the difficulty in slip transmission across grain boundaries.

The material volume between the indenter and the grain boundary confines the pileup of dislocations emitted from an indent. The slip localization and transfer into the next grain, resulting in grain boundary hardening, is strongly related to the distance between the indent and the grain boundary [24-27]. If an indentation is made too far from the boundary, the concentrated stress at the boundary will not reach the critical stress value needed for slip transfer. On the other hand, if the indent is too close, the indenter will cross the boundary before this value is reached. This effect is observed in the series of indents in Fig. 5.
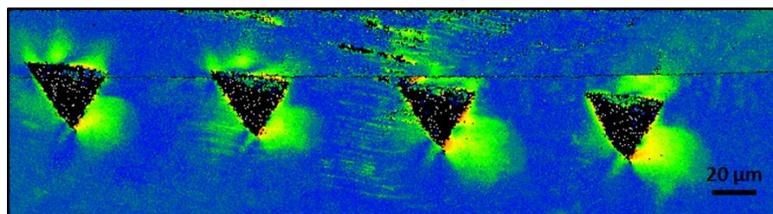

Figure 5: EBSD reference orientation-based misorientation map illustrates series of nano-indents crossing the same grain boundary, and resulting lattice rotation.

5. Summary

In the current study, optical and SEM imaging-based IC is employed to measure displacement fields at specimen-scale and microstructural-scale in Al-Cu specimens.

1) The full-field strain maps, along with information on underlying microstructure, obtained from the vicinity of grain boundaries and crack tips provide data needed for the calibration of CPFE models that currently rely on average specimen-scale behavior.

2) A complete analysis of the micro-structural details such as grain boundary planes, misorientations, active slip systems and local chemistry, affecting both slip transfer phenomena and crack tip interaction with a grain boundary, will provide new insights into deformation and microstructurally-sensitive fatigue cracking processes.

References

1. P.R. Dawson, Int. J. Solids Struct. 37 (2000) 115-130.
2. D. Raabe *et al.*, Acta Mater. 49 (2001) 3433-3441.
3. Matouš, K., Maniatty, A.M., Int. J. Numer. Meth. Engng. 60 (2004) 2313-2333.
4. J.D. Hochhalter *et al.*, Modell. Simul. Mater. Sci. Eng. 19 (2011) 035008.
5. S.R. Kalidindi, *et al.*, Adv. Mater. 15 (2003) 1345-1348.
6. F. Roters, *et al.*, Acta Mater. 58 (2010) 1152-1211.
7. F. Hild and S. Roux, Strain 42 (2006) 69-80.
8. M. Sutton, *et al.*, Image correlation for shape, motion and deformation measurements: Basic concepts, theory and applications. Springer, 2009.
9. A.M. Korsunsky, *et al.*, Int. J. Fatigue, 31 (2009) 1771-1779.
10. B. Pan, *et al.*, Meas. Sci. Technol. 20 (2009), 062001.
11. J.D. Carroll, *et al.*, Int. J. Fracture, 180 (2013) 1-19.
12. M. Tschopp, *et al.*, Met. Mater. Trans. A 40 (2009) 2363-2368.
13. Z. Zhou, *et al.*, Opt. Lasers Eng. 49 (2011) 366-370.
14. W. Zhang and Y. Liu, Int. J. Fatigue, 42 (2012) 14-23.
15. T.J. Turner, *et al.*, Modell. Simul. Mater. Sci. Eng. 21 (2013) 015002.
16. J.C. Schuren, *et al.*, Exp. Mech. 52 (2012), 461-479.
17. F. Delaire, *et al.*, Acta Mater. 48 (2000) 1075-1087.
18. N. Zhang and W. Tong, Int. J. Plasticity, 20 (2004) 523-542.
19. K.-S. Cheong and E.P. Busso, J. Mech. Phys. Sols. 54 (2006) 671-689.
20. S. Pathak, *et al.*, J. Mater. Sci. 47 (2012) 815-823.
21. M. Sutton, *et al.*, Exp. Mech. 47 (2007) 775-787.
22. M. Sutton, *et al.*, Exp. Mech. 47 (2007) 789-804.
23. V.K. Gupta and S.R. Agnew, Microsc. Microanal. 16 (2010) 831-841.
24. T. Ohmura, *et al.*, Mater. Trans. 46 (2005) 2026-2029.
25. W.A. Soer, *et al.*, Mater. Lett. 59 (2005) 3192-3195.
26. F.W. Herbert, *et al.*, MRS Proc. Vol. 1297, pp. mrsf10-1297, Camb. Univ. Press, 2011.
27. D. Faghihi and G.Z. Voyiadjis, Mech. Mater. 44 (2012) 189-211.